Strain relaxation and band-gap tunability in ternary $In_xGa_{1-x}N$ nanowires

H. J. Xiang,[1] Su-Huai Wei,[1,*] Juarez L. F. Da Silva,[1] and Jingbo Li[2,†]
[1]*National Renewable Energy Laboratory, Golden, Colorado 80401, USA*
[2]*State Key Laboratory for Superlattices and Microstructures, Institute of Semiconductors, Chinese Academy of Sciences, P.O. Box 912, Beijing 100083, People's Republic of China*

(Received 13 August 2008; revised manuscript received 1 October 2008; published 3 November 2008)

The alloy formation enthalpy and band structure of InGaN nanowires were studied by a combined approach of the valence-force field model, Monte Carlo simulation, and density-functional theory (DFT). For both random and ground-state structures of the coherent InGaN alloy, the nanowire configuration was found to be more favorable for the strain relaxation than the bulk alloy. We proposed an analytical formula for computing the band gap of any InGaN nanowires based on the results from the screened exchange hybrid DFT calculations, which in turn reveals a better band-gap tunability in ternary InGaN nanowires than the bulk alloy.

DOI: 10.1103/PhysRevB.78.193301 PACS number(s): 61.46.Km, 64.75.Op, 71.15.Mb, 71.22.+i

I. INTRODUCTION

The InGaN alloys have attracted great interest as they can be used to cover the emission spectral range from the ultraviolet to the near infrared by varying the InN composition. This makes InGaN an excellent candidate material for light emitting diodes,[1] laser diodes, and high-efficiency multijunction solar cells.[2] Unfortunately, for a composition of InN from ~15%–85%, spinodal decomposition occurs leading to the formation of In-rich and Ga-rich regions in InGaN, which have been attributed to the large lattice mismatch (~10%) between bulk InN and GaN.[3] Thus, there is a great effort to synthesize homogeneous InGaN alloys without phase separation.

A breakthrough was achieved recently by Kuykendall *et al.*[4] who synthesized single-crystalline $In_xGa_{1-x}N$ nanowires (NWs) across the entire compositional range ($0 \le x \le 1$) by low-temperature halide chemical vapor deposition.[4] The exceptional composition tunability was suggested to be due to the low process temperature and the ability of the NW morphology to accommodate strain-relaxed growth, which suppresses the tendency toward phase separation.[4] However, an atomic level understanding of the role of strain relaxation in alloy NWs is lacking, which is the key to understand the recent experiments. Furthermore, the knowledge of the electronic structure properties of the InGaN NWs is far from satisfactory, e.g., the dependence of the band gap of the alloy NWs as a function of In composition and NW diameter (D) remains unclear.

In order to address these issues, we employed atomic models to investigate the energetics and electronic properties of ternary $In_xGa_{1-x}N$ NWs. Our study provides direct evidence that the NW configuration is more favorable for strain release than the bulk $In_xGa_{1-x}N$ alloy, which explains the recent experimental observations.[4] Furthermore, an analytical formula for computing the band gap of alloy InGaN NWs with any diameters and In concentration was derived.

II. COMPUTATIONAL DETAILS

Due to the large system size involved in the alloy NW calculations, we employed a hierarchy approach, namely, valence-force field (VFF) model,[5–7] Monte Carlo (MC) simulations, and density-functional theory (DFT), to obtain reliable results with reduced computational cost. It is well known that for lattice-mismatched isovalent semiconductor alloys, the major contribution to the formation enthalpy is the strain energy. The strain energy could be described well by the VFF model[5–7] which considers the deviation of the nearest-neighbor bond lengths and bond angles from the ideal bulk InN and GaN values. The VFF parameters were taken from Refs. 8 and 9. In order to reduce the supercell that simulates the random InGaN alloy, the special quasirandom structure (SQS) model[10,11] was used. MC simulations were used for two purposes: (i) generate SQS for $In_xGa_{1-x}N$ NWs, in which the deviation of the correlation function from the one for ideal random alloy acts as the cost function; (ii) combined with the VFF model, it was used to determine the ground-state (GS) structures of the $In_xGa_{1-x}N$ NWs. For small NWs, DFT calculations within the local-density approximation (LDA) (Ref. 12) were performed in order to check the accuracy of the VFF method. It is well known that DFT with local or semilocal exchange-correlation functionals yields a negative fundamental band gap for InN,[13] instead of the recent experimental value of about 0.7 eV.[14] Therefore, in order to obtain a realistic description of the electronic structure of $In_xGa_{1-x}N$ NWs, we performed hybrid DFT calculations employing the screened Heyd-Scuseria-Ernzerhof 06 (HSE06) hybrid functional.[15–17] The DFT calculations were performed using the projected augmented wave (PAW) method[18] as implemented in the Vienna *ab initio* simulation package (VASP).[19] For the NWs, the surfaces were passivated by pseudohydrogen atoms.[20,21] In this work, the physical properties of $In_xGa_{1-x}N$ alloys were calculated at $x=0.5$ in which the alloy formation enthalpy is close to the maximum. The axis of NWs was chosen to be along the [0001] direction, as experimentally observed.[4]

III. $In_xGa_{1-x}N$ ALLOY STRUCTURES

As mentioned above, the random InGaN alloys were modeled by SQS structures,[10,11,22] where the cation sites are occupied by In or Ga atoms and the anion sites are occupied by N atoms in the wurtzite structure. Under coherent growth

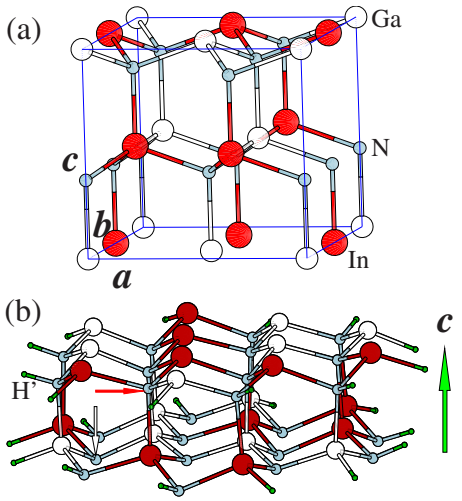

FIG. 1. (Color online) Lowest energy structures for (a) bulk $In_{0.5}Ga_{0.5}N$ alloy and (b) $In_{0.5}Ga_{0.5}N$ NW. Here red/gray or white arrows in (b) indicate two N atoms bonded with 3 In+1 Ga or 3 Ga+1 In.

condition, InGaN alloys can adopt the GS structure instead of the random ones at low temperature. With the VFF model, the enumeration of all possible structures of the alloy with 16 cations or less indicates that the structure shown in Fig. 1(a) is the GS structure for the bulk $In_{0.5}Ga_{0.5}N$ alloy.[23] In this configuration, each N atom bonds with two Ga and two In cations, which also occurs in the GS structure (chalcopyrite type) of the zinc-blende alloy.[24] It is noted that Fan *et al.*[25] suggested a GS structure of the wurtzite $A_{0.5}B_{0.5}C$ alloy from a search of possible structures within a fixed $2\times2\times2$ supercell.[25] Our LDA calculations showed that the global GS structure identified in this work has a lower energy by about 0.05 eV/4 atoms than the GS structure suggested by Fan *et al.*[25] We found that these two structures differ in their next-nearest-neighbor pair-correlation function despite of the same local environment of N atoms. MC simulations indicated that the structure shown in Fig. 1(b) is the GS structure for the NW.[26] Here, N atoms in the inner part of the NW have a similar bonding character as the bulk GS structure. However, there are two N atoms near the surface bonded with three In or three Ga atoms.

IV. FORMATION ENTHALPY

The formation enthalpy of isovalent semiconductor alloys $In_xGa_{1-x}N$ is defined as

$$\Delta H = E(x,\sigma) - [xE_{\mathrm{InN}}(a_{\mathrm{InN}}) + (1-x)E_{\mathrm{GaN}}(a_{\mathrm{GaN}})], \quad (1)$$

where E are the total energies and a_{InN} (a_{GaN}) is the equilibrium lattice constant for pure InN (GaN). Using the SQS and GS structures discussed above for the bulk and NW systems, we calculated the enthalpy formation using the VFF model and DFT-LDA methods. The results are reported in Table I. Using both methods, we found a smaller formation enthalpy for the NWs than for the bulk systems. As discussed before, the VFF method takes into account only the strain energy. Hence, strain release plays an important role for the lower formation enthalpy and thus the increased incorporation of In composition in NWs.

TABLE I. Alloy formation enthalpy (eV/4 atoms) of bulk $In_{0.5}Ga_{0.5}N$ alloy and $In_{0.5}Ga_{0.5}N$ NWs with a diameter around 1 nm.

	SQS (VFF)	SQS (DFT)	GS (VFF)	GS (DFT)
Bulk	0.165	0.198	0.075	0.053
NW	0.073	0.066	0.048	0.029

The experimental synthesized NWs have larger diameters than we discussed above.[4] Thus, to obtain further insight into the role played by the strain energy, we calculated the strain energy of $In_{0.5}Ga_{0.5}N$ NWs as a function of the diameter with the VFF model and SQS structures. The results are shown in Fig. 2. We found that the strain energy increases with diameter, as expected. We explain the results by using a simple core-shell model. In the core-shell model, the core part inside the shell part (with a width R_s nm) is similar to bulk. The use of this model is supported by the characteristic of our GS structure models for NW alloys [Fig. 1(b)]: the core part looks similar to the bulk case, while there are some differences in the outer part. Providing that the number of cations is proportional to the volume, the total strain energy (per four atoms) can be written as

$$E = E_c(R-R_s)^2/R^2 + E_s[R^2-(R-R_s)^2]/R^2, \quad (2)$$

where E_c and E_s are the strain energies of the core part and shell part, respectively. Here R is the effective radius of the NW defined as $R=[N_{\mathrm{NW}}\sqrt{3}/(2\pi)]^{1/2}a/2$, where N_{NW} is the number of atoms (not counting the surface pseudo-H atoms) of the NW with the unit length c and a is the average bulk lattice constant: $a=xa_{\mathrm{InN}}+(1-x)a_{\mathrm{GaN}}$. Fitting the calculated values with the core-shell model, we obtain $E_c=0.161$ eV/4 atoms, a much smaller $E_s=0.038$ eV/4 atoms, and $R_s=0.28$ nm. From Table I, we can see that E_c is indeed close to the energy of the bulk case (0.165 eV/4 atoms). As shown in Fig. 2, the dependence of the strain energy on the radius is well described by the core-shell model, which indicates that the better ability of accom-

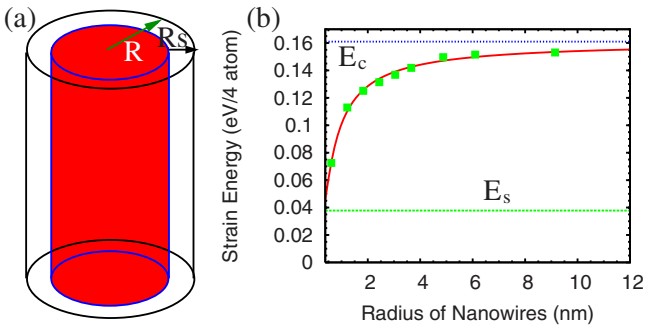

FIG. 2. (Color online) (a) Illustration for the core-shell model. (b) Strain energy dependence of $In_{0.5}Ga_{0.5}N$ NWs upon the radius of the NWs. The solid line is the fitted result according to the core-shell model [Eq. (2)]. The strain energies of the core part (E_c) and shell part (E_s) are indicated by horizontal lines.

TABLE II. Band gaps (E_g) and bowing parameters (b) of the $In_{0.5}Ga_{0.5}N$ alloy and related compounds. The diameters of the NWs are about 1 nm.

	E_g (eV)		b (eV)	
	LDA	HSE06	LDA	HSE06
Bulk GaN	2.127	3.445		
Bulk InN	−0.244	0.841		
Bulk GS $In_{0.5}Ga_{0.5}N$	0.776	1.909		
Bulk SQS $In_{0.5}Ga_{0.5}N$	0.527	1.674	1.66	1.88
NW GaN	3.660	5.143		
NW InN	1.538	2.574		
NW GS $In_{0.5}Ga_{0.5}N$	2.370	3.567		
NW SQS $In_{0.5}Ga_{0.5}N$	2.354	3.548	0.98	1.24

modating strain in NWs is mainly due to the large surface-to-volume ratio of NWs.

Based on the regular solution theory[3,27] and calculated formation enthalpy, we can estimate the critical temperature (T_c) above which the disorder alloy is formed. In this theory, the free energy (per cation) of mixing for $In_xGa_{1-x}N$ can be approximated as

$$\Delta G = \Omega x(1-x) + kT[x\ \ln(x) + (1-x)\ln(1-x)], \quad (3)$$

where the first and second terms are the mixing enthalpy and entropy contribution, respectively. Here the mixing enthalpy parameter Ω is diameter dependent and could be deduced from our above results for the $In_{0.5}Ga_{0.5}N$ NWs with different diameters. The critical temperature can then be calculated as $T_c = \frac{\Omega}{2k}$. From the formation enthalpy of the $In_{0.5}Ga_{0.5}N$ with the SQS structure, we can obtain Ω and thus T_c. Using the formation enthalpy predicted by the VFF model, $T_c(\mathrm{NW})/T_c(\mathrm{bulk}) = 0.44$ for the NW with $D = 1$ nm. DFT predicts an even smaller ratio $T_c(\mathrm{NW})/T_c(\mathrm{bulk}) = 0.33$. Ho and Stringfellow[3] predicted that $T_c(\mathrm{bulk}) = 1523$ K, T_c for $In_xGa_{1-x}N$ NWs can be much lower. However, we note that the above arguments are based only on the thermodynamic consideration. As mentioned by Kuykendall *et al.*,[4] the growth of $In_xGa_{1-x}N$ nanowires is not a fully equilibrium process. If we assume the growth occurs on the nanowire surface layer and atoms beneath the surface do not diffuse due to the low growth temperature, then the miscibility is determined by the strain energy of the shell part E_s; therefore large diameter homogeneous InGaN nanowires could be grown at low temperature.[4]

V. ELECTRONIC STRUCTURES

Now we turn to the discussion of the electronic properties of ternary InGaN alloys. The HSE06 band gaps of related nitrides are listed in Table II. For comparison, the results from the LDA calculations are also shown. Our calculations indicate that the HSE06 band gaps (3.445 and 0.841 eV, respectively) for bulk GaN and InN are in good agreement with the experimental values (3.47 and ~0.7 eV,[14] respectively). For NWs, the band gaps are larger than the corresponding bulk value as a result of quantum confinement: the LDA and HSE06 band gaps for the GaN (InN) NW with the diameter about 1.1 (1.3) nm are 3.660 and 5.143 (1.538 and 2.574) eV, respectively. For $In_xGa_{1-x}N$ alloys, the dependence of the band gap on the In concentration x can be described by a bowing parameter b.[28] Here, the bowing parameters are deduced from the band gaps of InN, GaN, and $In_{0.5}Ga_{0.5}N$. For the random bulk $In_{0.5}Ga_{0.5}N$ alloy, the gap bowing parameter extracted from the HSE06 band gaps is 1.88 eV. While for the $In_{0.5}Ga_{0.5}N$ NW, it is smaller by 0.64 eV than the bulk case. The LDA functional is found to reproduce the same trend of the bowing parameter as the HSE06 functional. The main difference is that the HSE06 bowing coefficients are larger by about 0.2 eV than the LDA values due to increased conduction-band state coupling. Lee and Wang[29] found similar increase in the bowing parameter in their screen-exchange local-density calculations on bulk cubic $In_xGa_{1-x}N$. We note that our LDA bowing parameter for bulk $In_{0.5}Ga_{0.5}N$ alloy is consistent with previous results obtained with the zinc-blende structure.[28,30]

Now we discuss how the band gap depends on the diameter D. It was shown that the band-gap difference (ΔE_g) between the NW and bulk can be described as[21] $\Delta E_g(D) = \beta/D^{\alpha}$. LDA calculations with modified pseudopotential[21] showed that $\alpha \approx 1.1$. Using this α value and the HSE06 band gaps for NWs, we obtain

$$\Delta E_g(D_1, \mathrm{InN}) = 2.27/D_1^{1.1},$$

$$\Delta E_g(D_2, \mathrm{GaN}) = 1.98/D_2^{1.1},$$

$$\Delta E_g(D_3, \mathrm{In_{0.5}Ga_{0.5}N}) = 2.31/D_3^{1.1}. \quad (4)$$

Here ΔE_g is in eV and D is in nm. From Eq. (4), we can obtain the bowing parameter $b(D)$ for $In_{0.5}Ga_{0.5}N$ NWs,

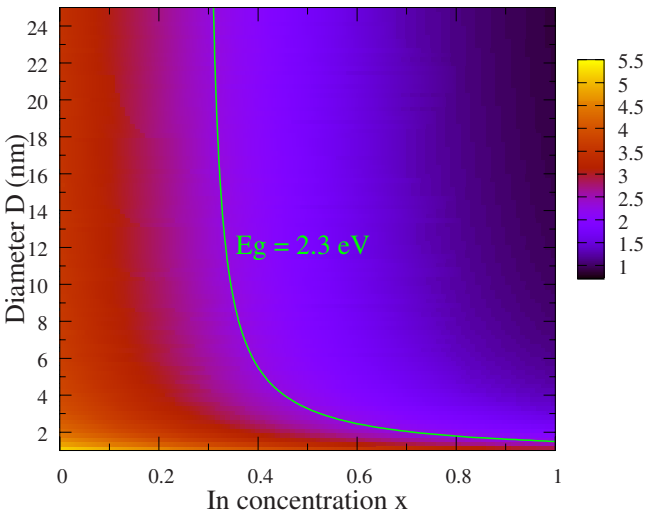

FIG. 3. (Color online) Estimated HSE06 band gaps (in eV) for $In_xGa_{1-x}N$ NWs with the diameters D using Eq. (6). The solid line is the contour line with $E_g = 2.3$ eV.

$$b(D_3, In_{0.5}Ga_{0.5}N) = -0.75/D_3^{1.1} + b_{bulk}, \quad (5)$$

where $b_{bulk}=1.88$ eV (see Table II).

Given the above results on the band gap of GaN, InN, and $In_{0.5}Ga_{0.5}N$ NWs, we can now estimate the band gap of an alloy $In_xGa_{1-x}N$ NW with any diameter D and x through the following formula:

$$\begin{aligned} E_g(D,x) &= xE_g(D_1,\mathrm{InN}) + (1-x)E_g(D_2,\mathrm{GaN}) \\ &\quad - b(D_3,In_{0.5}Ga_{0.5}N)x(1-x) \\ &= [1.98 + 0.75x - 0.71x^2]\left(\frac{1+0.111x}{D}\right)^{1.1} \\ &\quad + E_g(\mathrm{bulk},x), \end{aligned} \quad (6)$$

where D_1, D_2, and D_3 are the diameters of the corresponding InN, GaN, and $In_{0.5}Ga_{0.5}N$ NWs with the same N_{NW} as the $In_xGa_{1-x}N$ NW. The band gaps of $In_xGa_{1-x}N$ NW calculated as a function of x and D are shown in Fig. 3. Due to the quantum confinement effect, the band-gap tunability of the alloy NWs is better than the bulk alloy: not only the band gap extends to a larger range but also to obtain a given band gap, we can tune either the diameter or the In concentration of the alloy NW. For example, to achieve desirable green light emission at $E_g=2.3$ eV, we can use either an InN NW with a diameter about 1.5 nm or $In_{0.3}Ga_{0.7}N$ NW with a diameter larger than 25 nm, as shown in Fig. 3. For multijunction solar cell application, one can either use an In-rich tapered InGaN NWs (Ref. 4) or NWs with a constant diameter but with varying In concentration along the NW axis direction.

VI. CONCLUSION

In summary, our calculations identified the alloy structures of $In_{0.5}Ga_{0.5}N$ and demonstrated enhanced alloy solubility and band-gap tunability in ternary InGaN NWs.

ACKNOWLEDGMENTS

Work at NREL was supported by the U.S. Department of Energy under Contract No. DE-AC36-99GO10337. We thank G. Kresse for providing us the VASP 5.1 code. J.L. gratefully acknowledges financial support from the "One-Hundred Talents Plan" of the Chinese Academy of Sciences.

*suhuai_wei@nrel.gov
†jbli@semi.ac.cn

[1] J. W. Orton and C. T. Foxon, Rep. Prog. Phys. **61**, 1 (1998).
[2] J. Wu, W. Walukiewicz, K. M. Yu, W. Shan, J. W. Ager III, and E. E. Haller, J. Appl. Phys. **94**, 6477 (2003).
[3] I-hsiu Ho and G. B. Stringfellow, Appl. Phys. Lett. **69**, 2701 (1996).
[4] T. Kuykendall, P. Ulrich, S. Aloni, and P. Yang, Nature Mater. **6**, 951 (2007).
[5] P. Keating, Phys. Rev. **145**, 637 (1966).
[6] R. Martin, Phys. Rev. B **1**, 4005 (1970).
[7] J. L. Martins and A. Zunger, Phys. Rev. B **30**, 6217 (1984).
[8] S. Chen, X. G. Gong, and S.-H. Wei, Phys. Rev. B **77**, 073305 (2008).
[9] K. Kim, W. R. L. Lambrecht, and B. Segall, Phys. Rev. B **53**, 16310 (1996).
[10] A. Zunger, S.-H. Wei, L. G. Ferreira, and J. E. Bernard, Phys. Rev. Lett. **65**, 353 (1990).
[11] S.-H. Wei, L. G. Ferreira, J. E. Bernard, and A. Zunger, Phys. Rev. B **42**, 9622 (1990).
[12] J. P. Perdew and A. Zunger, Phys. Rev. B **23**, 5048 (1981); D. M. Ceperley and B. J. Alder, Phys. Rev. Lett. **45**, 566 (1980).
[13] C. Stampfl and C. G. Van de Walle, Phys. Rev. B **59**, 5521 (1999).
[14] J. Wu, W. Walukiewicz, K. M. Yu, J. W. Ager III, E. E. Haller, Hai Lu, William J. Schaff, Y. Saito, and Y. Nanishi, Appl. Phys. Lett. **80**, 3967 (2002).
[15] J. Heyd, G. E. Scuseria, and M. Ernzerhof, J. Chem. Phys. **118**, 8207 (2003).
[16] A. V. Krukau, O. A. Vydrov, A. F. Izmaylov, and G. E. Scuseria, J. Chem. Phys. **125**, 224106 (2006).
[17] J. Paier, M. Marsman, K. Hummer, G. Kresse, I. C. Gerber, and J. G. Ángyán, J. Chem. Phys. **124**, 154709 (2006).
[18] P. E. Blöchl, Phys. Rev. B **50**, 17953 (1994); G. Kresse and D. Joubert, *ibid.* **59**, 1758 (1999).
[19] G. Kresse and J. Furthmüller, Comput. Mater. Sci. **6**, 15 (1996); Phys. Rev. B **54**, 11169 (1996).
[20] H. J. Xiang and S.-H. Wei, Nano Lett. **8**(7), 1825 (2008).
[21] J. Li and L.-W. Wang, Phys. Rev. B **72**, 125325 (2005).
[22] Gan *et al.*, also provided a SQS structure for bulk $In_{0.5}Ga_{0.5}N$ alloy [C. K. Gan, Y. P. Feng, and D. J. Srolovitz, Phys. Rev. B **73**, 235214 (2006)].
[23] See EPAPS Document No. E-PRBMDO-78-148839 for the atomic coordinates of the unrelaxed GS structure of the bulk wurtzite $A_{0.5}B_{0.5}C$ alloy. For more information on EPAPS, see http://www.aip.org/pubservs/epaps.html.
[24] S.-H. Wei, L. G. Ferreira, and A. Zunger, Phys. Rev. B **41**, 8240 (1990).
[25] X. F. Fan, Z. Zhu, Y.-S. Ong, Y. M. Lu, Z. X. Shen, and Jer-Lai Kuo, Appl. Phys. Lett. **91**, 121121 (2007).
[26] In our simulations, we only considered coherent homogeneous structures along the [0001] direction, and the lattice constant of the NW is fixed to one c. For $In_{0.5}Ga_{0.5}N$ NWs with small diameters, the global ground state is the phase separated state with no broken bonds at the interface [see E. Ertekin, P. A. Greaney, D. C. Chrzan, and T. D. Sands, J. Appl. Phys. **97**, 114325 (2005)] as confirmed by our VFF calculations.
[27] A.-B. Chen and A. Sher, *Semiconductor Alloys: Physics and Materials Engineering* (Plenum, New York, 1995).
[28] F. Wang, S.-S. Li, J.-B. Xia, H. X. Jiang, J. Y. Lin, J. B. Li, and S.-H. Wei, Appl. Phys. Lett. **91**, 061125 (2007).
[29] B. Lee and L. W. Wang, J. Appl. Phys. **100**, 093717 (2006).
[30] L. Bellaiche, T. Mattila, L.-W. Wang, S.-H. Wei, and A. Zunger, Appl. Phys. Lett. **74**, 1842 (1999).